Scripta Materialia 242 (2024) 115904

Contents lists available at ScienceDirect

Scripta Materialia

journal homepage: www.journals.elsevier.com/scripta-materialia

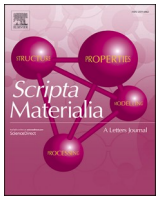

Compositional effects on strain-controlled actuation fatigue of NiTiHf high temperature shape memory alloys

A. Demblon, J.H. Mabe, I. Karaman *

Department of Materials Science and Engineering, Texas A&M University, College Station, TX 77843, United States

ARTICLE INFO

Keywords:
High-temperature shape memory alloys
Actuation fatigue
Partial transformation
Partial cycling
Thermal cycling

ABSTRACT

Nickel-rich NiTiHf high-temperature shape memory alloys continue to garner significant interest for actuator applications. One issue impeding their widespread use is the question of actuation fatigue lifetime under high loads. This paper describes how these fatigue challenges can be overcome by partial thermomechanical cycling. By limiting actuation strain to less than the maximum value that is attainable with full transformation, actuation life cycles can be significantly extended. Strain-controlled cycling is achieved by limiting the upper cycle temperature during heating and stopping each cycle short of the austenite finish temperature. Four compositions of NiTiHf were tested to three levels of transformation. Strain-controlled cycling increased the actuation fatigue lifetimes of all compositions. However, specimens resistant to dislocation plasticity attained longer lives during full transformation cycling, but during partial cycling, they failed earlier than samples with higher resistance to plasticity. This highlights the importance of the competition between functional and structural fatigue.

Nickel-rich NiTiHf high-temperature shape memory alloys (HTSMAs) are better alternatives to the conventional binary NiTi alloys in solid-state actuator applications due to their higher transformation temperatures (TTs), increased work output, and improved stability. Increased work output stems from the higher strength and stability of Ni-rich NiTiHf HTSMAs permitting larger service loads. However, this comes at the expense of the number of actuation cycles to failure. Many studies have focused on solving the short-lifetime issue by fine-tuning the microstructure during alloy fabrication and processing [1–6]. Although this is a viable approach, consistent SMA fabrication in general is difficult and this difficulty is compounded by the compositional sensitivity of Ni-rich NiTiHf alloys [6,7]. As an alternative to the difficulty of composition and processing control for an extended actuation lifecycle, this study focuses on developing a fundamental understanding of the effects of various operational conditions and cycling parameters on the actuation fatigue response. This provides an approach to optimize the actuation performance across multiple compositions compensating for variations in material fabrication and processing. In NiTiHf HTSMAs, the effects of applied load [8] and operating temperature [9], and in NiTi SMAs, the effects of heating/cooling rates [10,11] and heating waveform [12] on actuation fatigue responses have been well documented for full transformation cycling. Yet the effects of strain-controlled actuation fatigue response of SMAs, in general, have not been studied in detail, let alone NiTiHf HTSMAs. This is becoming more important with the increasing number of proposed implementations and applications for SMA actuators. In many SMA actuator applications, strain-controlled thermomechanical cycling can be used to meet all the operational load and displacement requirements, while avoiding the detrimental effects of full transformation cycling.

To the best of the authors' knowledge, there are only a few investigations on the strain-controlled (also known as partial) thermomechanical fatigue cycling of SMAs with only two of these on NiTiHf HTSMAs [11,13–18]. In these studies, no experiments were conducted to see if the strain-controlled actuation fatigue responses differ across various compositions. Hence, this work is focused on determining the compositional effects on strain-controlled actuation fatigue of Ni-rich NiTiHf HTSMAs, with a special emphasis on the competition between functional and structural fatigue responses. Structural fatigue is the development of irrevocable damage leading to crack generation and eventually rupture, whereas functional fatigue is described by the cyclic evolution or degradation of transformation characteristics (e.g. transformation temperatures, strains and hysteresis) beyond a usable limit [19].

Four materials were used in this investigation with the following nominal compositions: $Ni_{50.5}Ti_{33.5}Hf_{16}$, $Ni_{50.6}Ti_{30.4}Hf_{19}$, and two different production lots or batches of $Ni_{50.3}Ti_{29.7}Hf_{20}$ (in atomic

* Corresponding author.
E-mail address: ikaraman@tamu.edu (I. Karaman).

https://doi.org/10.1016/j.scriptamat.2023.115904
Received 29 July 2023; Received in revised form 5 November 2023; Accepted 26 November 2023
Available online 13 December 2023

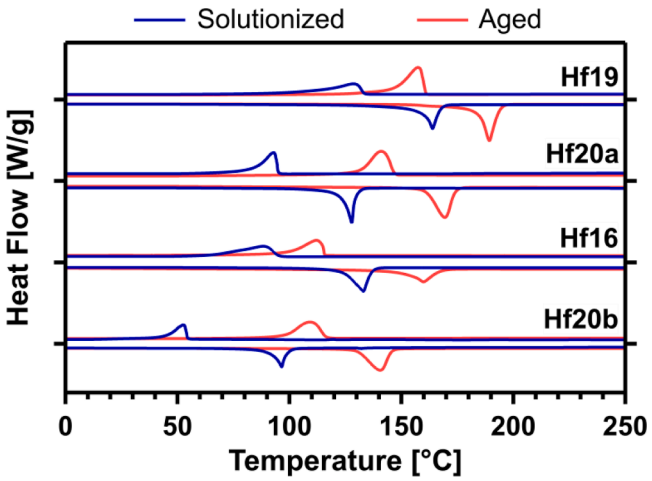

Fig. 1. DSC curves for the four NiTiHf HTSMAs used in this work after a 900 °C-1hr WQ solution heat treatment (blue) and 550 °C-3hr AC (red) aging heat treatment.

percent). The $Ni_{50.5}Ti_{33.5}Hf_{16}$ and $Ni_{50.6}Ti_{30.4}Hf_{19}$ alloys, referred to as Hf16 and Hf19 herein, were both melted by plasma arc melting and hot extruded at 900 °C to a 9:1 area reduction ratio. The $Ni_{50.3}Ti_{29.7}Hf_{20}$ alloys, referred to as Hf20a and Hf20b, were both vacuum induction skull melted and hot extruded at 900 °C to a 6:1 area reduction ratio. Although the Hf20a and Hf20b alloys were intended to have the same composition and the raw element feedstocks were mixed to the same ratio, they were melted in different batches and have been shown in previous studies [1] to have different final compositions.

The transformation temperatures of each material were measured using a TA Instruments Q2000 differential scanning calorimeter (DSC) with a heating/cooling rate of 10 °C/min. Small 3 mm diameter DSC samples were cut using wire electrical discharge machining (EDM). The results are shown in Fig. 1 for solutionized (blue) and aged (red) samples, and the measured TTs from these curves are given in Table 1. Solutionizing was performed at 900 °C-1hr followed by water quenching (WQ). To prevent oxidation, these samples were sealed in evacuated quartz tubes with a Ti sponge oxygen getter and back filled with high purity argon. The purpose of this treatment is to produce precipitate free material so that the TTs measured via DSC are indicative of the actual relative compositions which are known to vary considerably from their nominal values when producing large melts of NiTiHf material [1,20].

It is known that higher Hf content increases TTs whereas higher Ni content decreases them, and variations in Ni content have a much greater impact on TTs than Hf [7]. It can be inferred that any differences in actual composition from nominal composition, as indicated by shifted DSC curves (as demonstrated by Hf20a and Hf20b), are primarily due to differences in Ni content. Hence, assuming the Hf content of each batch is close to the nominal composition Hf20b has more Ni than Hf20a. Likewise, Hf19 has a lower Ni content than that of Hf20a as the Hf contents are somewhat similar. As Hf16 has a significantly lower Hf content, the decrease in TTs may be simply due to the lower Hf content, thus, Ni content in Hf16 is either the same or slightly lower than that of Hf19. Comparing the solutionized M_s temperatures to those presented in the systematic study on the effects of Ni and Hf content on TTs by Umale et al. [7] the actual Ni contents of Hf16, Hf19, Hf20a, and Hf 20b are likely closer to 50.55 at.%, 50.68 at.%, 50.84 at.%, and 50.92 at.%, respectively. Before actuation fatigue testing the samples were peak aged at 550 °C for 3hr in air and air cooled (AC) to precipitate strengthen the alloys and the aged TTs are listed in Table 1.

Characterization of impurities was carried out using a Tescan LYRA-3 Model GMH scanning electron microscope (SEM). SEM samples were mechanically polished to 1200 grit followed by a 3 μm silica slurry. Back scattered electron (BSE) images were taken of the samples and analyzed in FIJI [21] to determine the amount of non-metallic inclusions (NMIs) in each material. The BSE SEM images in Fig. 2a show relative size and distribution of the impurities found in each material. The analysis of these images is given in Fig. 2b detailing the relative area fraction of impurities and their mean particle size from each alloy. One can see that Hf16 had the highest level of large inclusions at ~0.6 area% with an average size of ~1.2 μm^2. Hf19, Hf20a and Hf20b were similar to each other with a significantly lower inclusion fraction (~0.2 area%). However, Hf20a and Hf20b had an average inclusion size of ~0.9 μm^2 and Hf19 had the smallest inclusions with the size of ~0.5 μm^2. Energy dispersive X-ray spectroscopy (EDS) was employed to examine the chemical composition of the observed impurities which were determined to be a mixture of HfO_2 (white particles) and $(Ti+Hf)_4Ni_2O_x$ (black particles). Note that the amount of NMIs affects the actuation fatigue lives NiTiHf HTSMAs by impacting their structural fatigue response [1,18].

Transmission electron microscopy (TEM) was performed using an FEI Tecnai F20 ST FEG instrument to determine the size and distribution of H-phase precipitates after aging (Fig. 2c). Fig. 2d represents the calculated mean precipitate length and width in each aged composition. It can be seen in these figures that Hf16 has a sparse heterogenous distribution of larger precipitates (~32 μm long and ~15 μm wide), whereas those in Hf19, Hf20a, and Hf20b are all homogenously distributed with a similar small size (~15 μm long and ~7 μm wide). In Fig. 2c the H-phase content of Hf20b appears more numerous and densely packed than the other alloys. H-phase precipitates are rich in Ni and Hf and poor in Ti as compared to the precipitate free matrix composition [22,23]. It has been shown that nucleation of these precipitates is governed by Ni diffusion and precipitate coarsening depends on Hf diffusion [24–26]. Hence, a higher Ni-content results in higher number of H-phase particles as is demonstrated in the Hf20 alloys with the most precipitates and highest Ni content. Conversely, Hf16 has the lowest amount of Ni and Hf resulting in nucleating and preferentially growing only a few precipitates.

Table 1
Transformation temperatures after a solution heat treatment of 900 °C-1hr water quenched and aging heat treatment of 550 °C-3hr air cooled for the four NiTiHf alloys used in this study.

Material	Heat Treatment	Transformation Temperatures [°C]				Hysteresis [°C]
		M_f	M_s	A_s	A_f	A_f–M_s
Hf16	900 °C-1hr WQ	88	98	138	151	53
	550 °C-3hr AC	99	116	145	169	53
Hf19	900 °C-1hr WQ	106	133	156	168	35
	550 °C-3hr AC	144	161	182	195	34
Hf20a	900 °C-1hr WQ	83	95	122	131	36
	550 °C-3hr AC	126	140	157	168	28
Hf20b	900 °C-1hr WQ	44	54	89	103	49
	550 °C-3hr AC	98	116	130	146	30

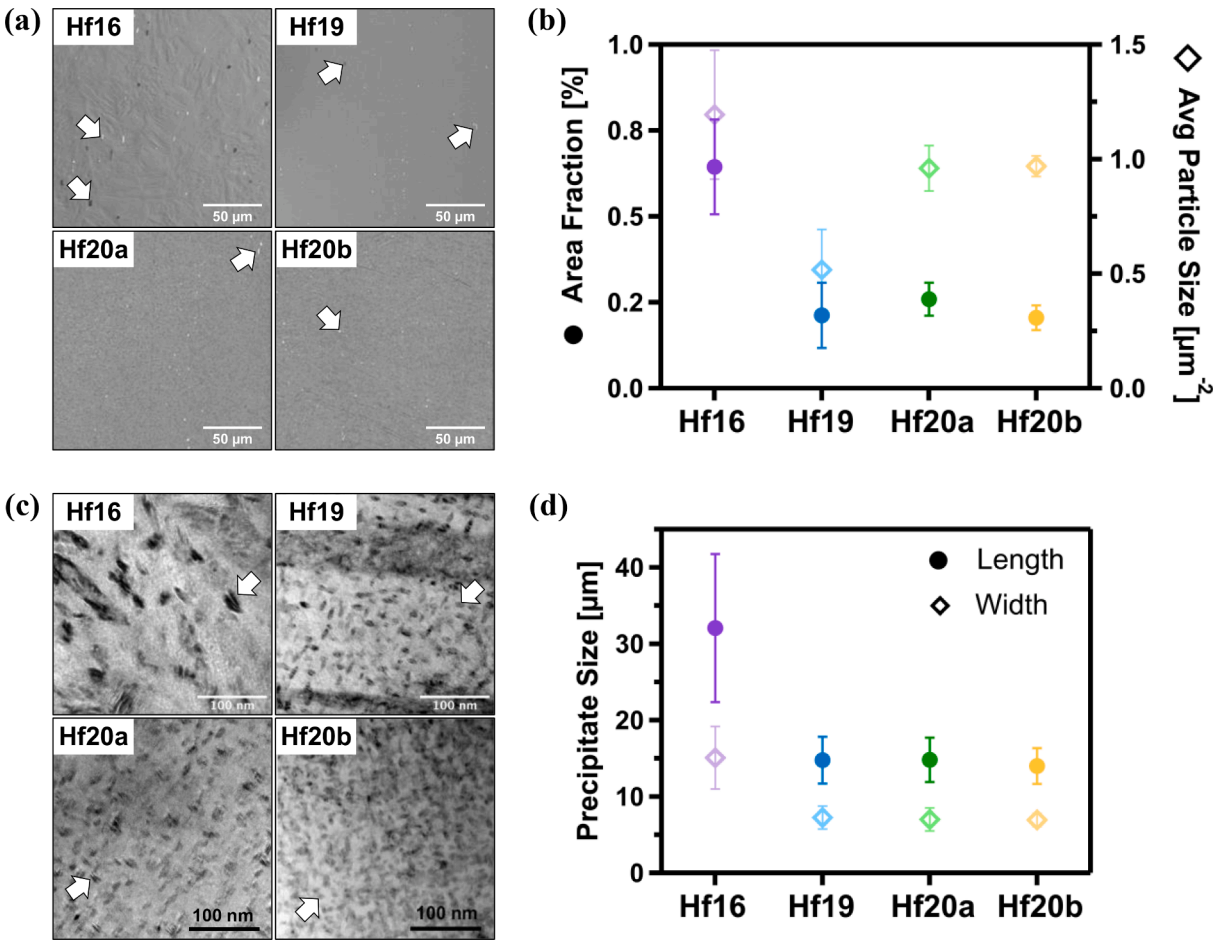

Fig. 2. Material characterization results showing: (a) Back scattered electron (BSE) SEM images showing the HfO_2 and $(Ti+Hf)_4Ni_2O_x$ (black) particles present in each material (emphasized by white arrows). (b) The area fraction (solid circles) and average particle size (hollow diamonds) of non-metallic inclusions for the four materials calculated from the BSE images of multiple regions of each specimen. (c) the bright-field TEM images showing the dark H-phase precipitates (emphasized by white arrows) present in each NiTiHf composition after aging at 550 °C-3 h. (d) The mean H-phase precipitate length and width measured from the TEM images.

Actuation fatigue dog bone samples were wire EDM cut from each of the materials, aged at 550 °C-3 hrs in air followed by air cooling, and tested in a custom tensile actuation fatigue frame [18]. The details of the experimental set up and how the actuation fatigue experiments performed can be found in [1,18]. All samples were tested under a constant force with an initial stress of 300 MPa up to three different degrees of transformation: 100–0 % martensite volume fraction (MVF), 100–25 % MVF, and 100–50 % MVF. Fig. 3 defines full transformation cycling (100–0 % MVF) versus partial transformation cycling (100-X% MVF). Full transformation cycles were performed by cycling samples between a lower cycle temperature (LCT) below martensite finish (M_f) and an upper cycle temperature (UCT) above austenite finish (A_f). For each test, the samples were initially run for 100 cycles at 300 MPa under full transformation (below M_f to above A_f) to stabilize actuation and determine the maximum attainable actuation strain (ε_{act}). After 100 cycles the samples were cooled to the LCT and for all subsequent cycles they were heated to a partial upper cycle temperature (PUCT) until the desired fraction of maximum ε_{act} was reached (75 % or 50 %), labelled ε_{PUCT}. They were then cycled to failure while holding the ε_{act} level constant by limiting the maximum sample temperature on each cycle. Actuation strain is the difference between the strain measured at the LCT (ε_{LCT}) and that at the UCT (ε_{UCT}) or ε_{LCT} - ε_{PUCT} for partial cycles. As the samples were cycled, the upper temperature for each cycle tended to increase as the test frame maintained a constant ε_{act}. To ensure the validity of the results each condition was repeated at least twice. Each test took between 10 and 26 days to complete.

The fatigue lives for each material and test case are summarized in Fig. 4 with 100–0 %, 100–25 %, and 100–50 % MVF represented by blue, green, and orange bars correspondingly. Under full transformation (100–0 % MVF) Hf16 survived the longest at 4500 ± 515 cycles. The other materials only lasted 3264 ± 364 cycles, 2265 ± 372 cycles, and 1420 ± 194 cycles in Hf19, Hf20a and Hf20b respectively. An initial assumption prior to strain-controlled partial cycling was that alloys with the longest actuation lifetime during full cycling would also have the longest partial cycling actuation lifetime. However, as can be seen in Fig. 4, this is not the case. In fact, the alloys with the shortest fatigue lives under full transformation, Hf20a and Hf20b, had the greatest increase in life due to the strain-controlled actuation fatigue testing. At 50 % transformation, Hf20a had a 15x increase and Hf20b had a 20x increase in lifetime from that attained under full cycling, compared to Hf16 and Hf19 which had a mere 4x and 7x rise in lifetime at 50 % actuation.

Fig. 5 displays the cyclic evolution of the actuation strain (ε_{act}) (i) and LCT strain (ε_{LCT}) (ii) for all materials at the three tested levels of full and partial transformation (a. 100 %, b. 75 %, and c. 50 %). Irrecoverable strain (UCT strain) is not shown since the partially cycled samples are not heated above A_f. However, ε_{LCT} evolution can also indicate the evolution of transformation induced plasticity (TRIP). TRIP is known to contribute to the formation of cracks during actuation fatigue [27–29]. Typically, NiTiHf with less resistance to dislocations (“soft” alloys) have a greater initial accumulation of TRIP leading to longer actuation fatigue lives by postponing the structural fatigue damage (crack) accumulation.

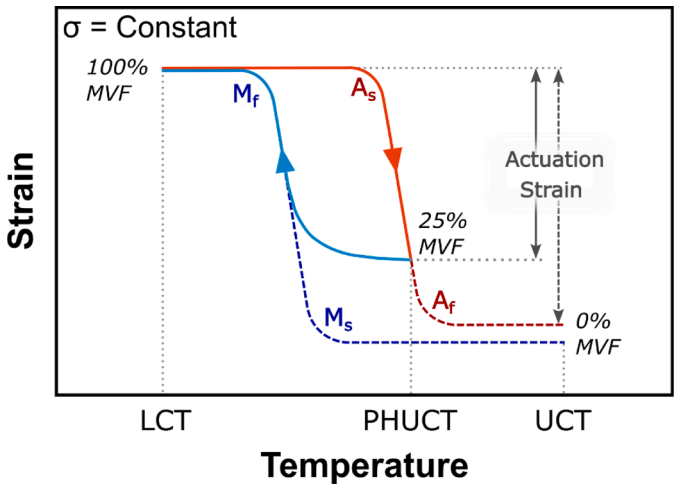

Fig. 3. Schematic of a typical strain vs. temperature plot for SMAs under a constant force. The blue lines correspond to cooling from austenite to martensite and the red lines correspond to heating from martensite to austenite. The dashed lines are representative of full cycling between a lower cycle temperature (LCT) and an upper cycle temperature (UCT). The solid lines represent a partial heating cycle, heating from the LCT to a partial heating UCT (PHUCT) until the desired fraction of actuation is attained. M_f, M_s, A_s, and A_f correspond to the transformation temperatures at the applied load σ. The actuation strain during full cycling and partial cycling are calculated as the difference between the strain at the LCT and the UCT or PHUCT during heating.

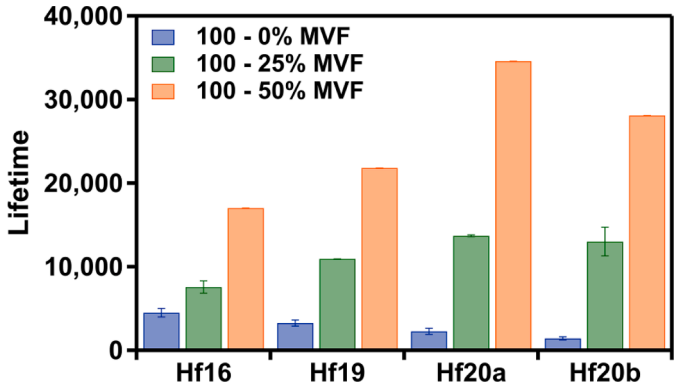

Fig. 4. Summary of the actuation fatigue lives of each of the four tested NiTiHf compositions cycled to three degrees of transformation to failure (100 %, 75 %, and 50 %).

This is because the build-up of plastic deformation creates regions of retained martensite which reduces the total transforming volume resulting in less ε_{act} and more functional fatigue. With a smaller volume to further generate dislocations there are fewer high stress regions for crack nucleation. Because the UCT remains constant in the 100–0 % MVF (full transformation) condition there is no subsequent increase in driving force to compel these retained areas to transform. This is illustrated by the steep increase in ε_{LCT} and longer lifetimes under full transformation (Fig. 5aii) for the Hf16 and Hf19 samples.

Conversely, materials with a high resistance to plastic deformation do not generate TRIP readily and create less retained martensite providing better functional fatigue than soft alloys. However, high resistance to plastic deformation promotes more complete transformation under full cycling (with a fixed UCT) which increases the amount of high stress regions for crack nucleation reducing structural fatigue. This is indicated by the relatively smaller increases in ε_{LCT} evolution but shorter lifetimes (Fig. 5aii) for the Hf20a and Hf20b specimens.

Strain-controlled actuation cycling increases fatigue lives (as compared to full cycling) by reducing the amount of crack initiation and reducing the structural fatigue damage accumulation. The reduction in crack initiation is caused by a shift in transformation regions as dislocations accumulate in preferential areas and impede transformation to a point that alternate zones become preferential transformation regions [18]. NiTiHf HTSMAs that are less resistance to plastic deformation accelerate the process of moving preferential transformation zones developing a larger number of interfaces (austenite/martensite and martensite/martensite) for damage to occur. In addition, the more rapidly raising required global transformation driving force present in softer materials (i.e. higher UCT as compared to compositions with higher plasticity resistance) forces transformation in high TRIP regions further promoting crack nucleation. Hence, Hf16 and Hf19 have an increased lifetime under strain-controlled actuation fatigue experiments but not as significantly as Hf20a and Hf20b.

NiTiHf HTSMAs exhibit solution strengthening as larger Hf atoms substitute Ti atoms in the Ti sub-lattice [30] and precipitate strengthening due to the formation of H-phase precipitates upon aging [23]. Hf16 had the least resistance to plastic deformation due to its low Ni and Hf content and sparse heterogenous distribution of H-phase not providing optimal solution or precipitate strengthening. Hf19 had the second lowest plastic deformation resistance due to lower Ni content and sparser H-phase than Hf20a and Hf20b. Hf20a and Hf20b are very similar, however, the lower fatigue life observed in Hf20b could be attributed to being highly Ni-rich and having very dense precipitation which both make the alloy more susceptible to rapid crack growth and rupture.

The amounts of NMIs in the tested alloys do not appear to have impacted the observed actuation fatigue results substantially. Hf16 had the highest impurity content, yet, it was the softest of the alloys and it has been shown that actuation fatigue is less affected by inclusions in softer materials [1]. Further evidence is that Hf19, Hf20a, and Hf20b all had a similar and very low impurity area fraction and Hf19 still had a poorer partial cycling actuation fatigue life than the Hf20 alloys.

In summary, the effects of composition on the strain-controlled actuation fatigue response of Ni-rich NiTiHf HTSMAs were investigated in the present study. Main findings and conclusions can be summarized as follows:

- Strain controlled actuation fatigue experiments via partial austenite transformation increases the actuation fatigue lifetimes of Ni-rich NiTiHf HTSMAs as compared to those for full austenite transformation.
- Lower Ni, Hf, and H-phase contents decrease the resistance to dislocation plasticity in NiTiHf HTSMAs leading to extensive TRIP, which positively impacts the structural fatigue response under full transformation cycles but leads to a poor functional fatigue response and substantial deterioration of actuation strain.
- Lower resistance to dislocation plasticity in Hf16 and Hf19 alloys reduces the benefits of strain-controlled actuation fatigue testing (i.e. partial austenite transformation) by causing a more rapid evolution of the transforming volume during partial cycling which increases the required global transformation driving force as well as the number of interfaces which act as crack nucleation sites.

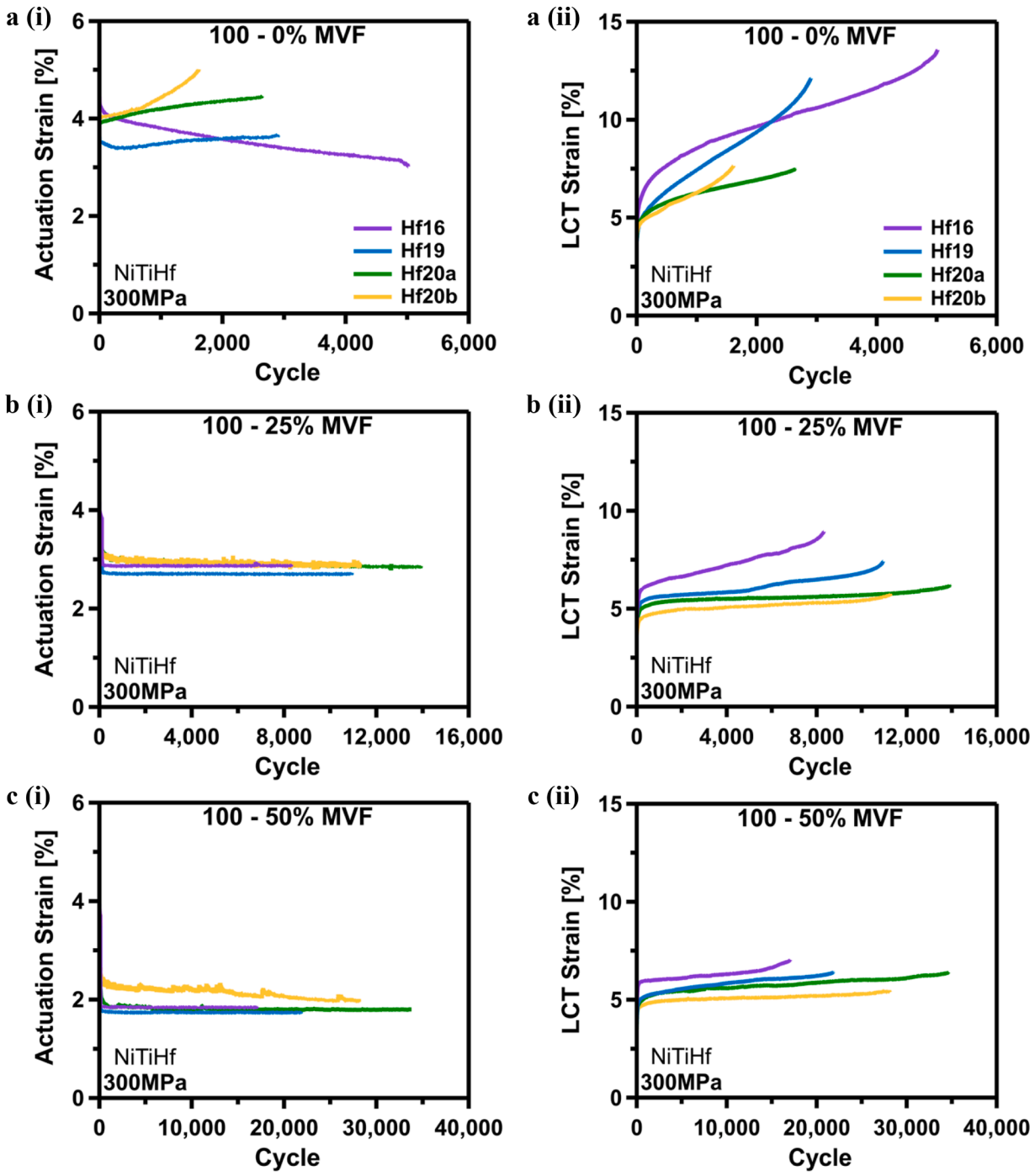

Fig. 5. Cyclic evolution of (i) actuation strain (ε_{act}), and (ii) LCT strain (ε_{LCT}) until sample rupture. The ε_{act} and ε_{LCT} evolutions are compared between the three test conditions; (a) 100–0 % MVF, (b) 100–25 % MVF, and (c) 100–50 % MVF.

- The detrimental effect of non-metallic inclusions is less severe in compositions with a lower resistance to dislocation plasticity or compositions undergoing partial austenite thermal cycling.

Declaration of Competing Interest

The authors declare that they have no known competing financial interests or personal relationships that could have appeared to influence the work reported in this paper.

Acknowledgements

The authors would like to acknowledge the financial support from the NASA University Leadership Initiative, under Grant No. NNX17AJ96A, and US National Science Foundation, Grant No. CMMI-1917367 and DMR-2004752. Use of the TAMU Materials Characterization Core Facility is acknowledged (RRID:SCR_022202) for SEM and TEM imaging.

References

[1] A. Demblon, O. Karakoc, J. Sam, D. Zhao, K.C. Atli, J.H. Mabe, I. Karaman, Compositional and microstructural sensitivity of the actuation fatigue response in NiTiHf high temperature shape memory alloys, Mater. Sci. Eng. A 838 (2022), 142786.

[2] O. Karakoc, C. Hayrettin, A. Evirgen, R. Santamarta, D. Canadinc, R. Wheeler, S. Wang, D. Lagoudas, I. Karaman, Role of microstructure on the actuation fatigue performance of Ni-Rich NiTiHf high temperature shape memory alloys, Acta Mater. 175 (2019) 107–120.

[3] B. Kockar, I. Karaman, A.V. Kulkarni, Y. Chumlyakov, I.V. Kireeva, Effect of severe ausforming via equal channel angular extrusion on the shape memory response of a NiTi alloy, J. Nucl. Mater. 361 (2007) 298–305.

[4] A. Kreitcberg, V. Brailovski, S. Prokoshkin, Y. Facchinello, K. Inaekyan, S. Dubinskiy, Microstructure and functional fatigue of nanostructured Ti–50.26at% Ni alloy after thermomechanical treatment with warm rolling and intermediate annealing, Mater. Sci. Eng. A 562 (2013) 118–127.

[5] K.C. Atli, I. Karaman, R.D. Noebe, G. Bigelow, D. Gaydosh, Work production using the two-way shape memory effect in NiTi and a Ni-rich NiTiHf high-temperature shape memory alloy, Smart Mater. Struct. (12) (2015) 24.

[6] O. Benafan, G.S. Bigelow, A. Garg, R.D. Noebe, D.J. Gaydosh, R.B. Rogers, Processing and scalability of NiTiHf high-temperature shape memory alloys, Shape Mem. Superelasticity 7 (1) (2021) 109–165.

[7] T. Umale, D. Salas, B. Tomes, R. Arroyave, I. Karaman, The effects of wide range of compositional changes on the martensitic transformation characteristics of NiTiHf shape memory alloys, Scr. Mater. 161 (2019) 78–83.

[8] O. Karakoc, C. Hayrettin, D. Canadinc, I. Karaman, Role of applied stress level on the actuation fatigue behavior of NiTiHf high temperature shape memory alloys, Acta Mater. 153 (2018) 156–168.

[9] O. Karakoc, C. Hayrettin, M. Bass, S. Wang, D. Canadinc, J. Mabe, D. Lagoudas, I. Karaman, Effects of upper cycle temperature on the actuation fatigue response of NiTiHf high temperature shape memory alloys, Acta Mater. 138 (2017) 185–197.

[10] O. Akgul, H.O. Tugrul, B. Kockar, Effect of the cooling rate on the thermal and thermomechanical behavior of NiTiHf high-temperature shape memory alloy, J. Mater. Res. 35 (12) (2020) 1572–1581.

[11] G. Scirè Mammano, E. Dragoni, Effect of stress, heating rate, and degree of transformation on the functional fatigue of Ni-Ti shape memory wires, J. Mater. Eng. Perform. 24 (7) (2015) 2709–2719.

[12] R. Casati, A. Tuissi, Effect of current pulses on fatigue of thin NiTi wires for shape memory actuators, J. Mater. Eng. Perform. 21 (12) (2012) 2633–2637.

[13] S. Ganesan, S. Vedamanickam, Effect of operating parameters on functional fatigue characteristics of an Ni-Ti shape memory alloy on partial thermomechanical cycling, J. Intell. Mater. Syst. Struct. (2022).

[14] H.O. Tugrul, H.H. Saygili, B. Kockar, Influence of limiting the actuation strain on the functional fatigue behavior of Ni50.3Ti29.7Hf20 high temperature shape memory alloy, J. Intell. Mater. Syst. Struct. 32 (2) (2020) 219–227.

[15] M. Karhu, T. Lindroos, Long-term behaviour of binary Ti–49.7Ni (at.%) SMA actuators—the fatigue lives and evolution of strains on thermal cycling, Smart Mater. Struct. (11) (2010) 19.

[16] D.C. Lagoudas, D.A. Miller, L. Rong, P.K. Kumar, Thermomechanical fatigue of shape memory alloys, Smart Mater. Struct. 18 (8) (2009).

[17] O.W. Bertacchini, D.C. Lagoudas, E. Patoor, Thermomechanical transformation fatigue of TiNiCu SMA actuators under a corrosive environment – part I: experimental results, Int. J. Fatigue 31 (10) (2009) 1571–1578.

[18] A. Demblon, J.H. Mabe, I. Karaman, Order of Magnitude Increase in Actuation Fatigue Lifetime Through Partial Austenitic Transformation of NiTiHf High Temperature Shape Memory Alloys, Department of Materials Science and Engineering, College of Engineering, Texas A&M University, 2023 [Manuscript submitted for publication].

[19] G. Eggeler, E. Hornbogen, A. Yawny, A. Heckmann, M. Wagner, Structural and functional fatigue of NiTi shape memory alloys, Mater. Sci. Eng. A 378 (1) (2004) 24–33.

[20] O. Benafan, G.S. Bigelow, A. Garg, R.D. Noebe, D.J. Gaydosh, R.B. Rogers, Processing and scalability of NiTiHf high-temperature shape memory alloys, Shape Mem. Superelasticity (2021).

[21] J. Schindelin, I. Arganda-Carreras, E. Frise, V. Kaynig, M. Longair, T. Pietzsch, S. Preibisch, C. Rueden, S. Saalfeld, B. Schmid, J.Y. Tinevez, D.J. White, V. Hartenstein, K. Eliceiri, P. Tomancak, A. Cardona, Fiji: an open-source platform for biological-image analysis, Nat. Methods 9 (7) (2012) 676–682.

[22] X.D. Han, R. Wang, Z. Zhang, D.Z. Yang, A new precipitate phase in a TiNiHf high temperature shape memory alloy, Acta Mater. 46 (1) (1998) 273–281.

[23] F. Yang, D.R. Coughlin, P.J. Phillips, L. Yang, A. Devaraj, L. Kovarik, R.D. Noebe, M.J. Mills, Structure analysis of a precipitate phase in an Ni-rich high-temperature NiTiHf shape memory alloy, Acta Mater. 61 (9) (2013) 3335–3346.

[24] M. Prasher, D. Sen, J. Bahadur, R. Tewari, M. Krishnan, Correlative SANS and TEM investigation on precipitation kinetics of H-phase in Ni50.3Ti29.7Hf20 high temperature shape memory alloy, J. Alloys Compd. 779 (2019) 630–642.

[25] R. Santamarta, R. Arróyave, J. Pons, A. Evirgen, I. Karaman, H.E. Karaca, R. D. Noebe, TEM study of structural and microstructural characteristics of a precipitate phase in Ni-rich Ni–Ti–Hf and Ni–Ti–Zr shape memory alloys, Acta Mater. 61 (16) (2013) 6191–6206.

[26] A. Shuitcev, Y. Ren, B. Sun, G.V. Markova, L. Li, Y.X. Tong, Y.F. Zheng, Precipitation and coarsening kinetics of H-phase in NiTiHf high temperature shape memory alloy, J. Mater. Sci. Technol. 114 (2022) 90–101.

[27] P.S. Chaugule, O. Benafan, J.B. le Graverend, Phase transformation and viscoplasticity coupling in polycrystalline nickel-titanium-hafnium high-temperature shape memory alloys, Acta Mater. 221 (2021), 117381.

[28] Y. Zhang, X. Chai, X. Ju, Y. You, S. Zhang, L. Zheng, Z. Moumni, J. Zhu, W. Zhang, Concentration of transformation-induced plasticity in pseudoelastic NiTi shape memory alloys: insight from austenite–martensite interface instability, Int. J. Plast. 160 (2023), 103481.

[29] Y. Zhang, Z. Moumni, Y. You, W. Zhang, J. Zhu, G. Anlas, Multiscale TRIP-based investigation of low-cycle fatigue of polycrystalline NiTi shape memory alloys, Int. J. Plast. 115 (2019) 307–329.

[30] M. Prasher, D. Sen, R. Tewari, P.S.R. Krishna, P.D. Babu, M. Krishnan, Effect of Hf solute addition on the phase transformation behavior and hardness of a Ni-rich NiTi alloy, Mater. Chem. Phys. 247 (2020), 122890.